

Dielectric Response of Nanoscopic Spherical Colloids in Alternating Electric Fields: A Dissipative Particle Dynamics Simulation

Jiajia Zhou and Friederike Schmid

Institut für Physik, Johannes Gutenberg-Universität Mainz,
Staudingerweg 7, D-55099 Mainz, Germany

E-mail: zhou@uni-mainz.de and friederike.schmid@uni-mainz.de

Abstract. We study the response of single nanosized spherical colloids in electrolyte solution to an alternating electric field (AC field) by computer simulations. We use a coarse-grained mesoscopic simulation approach that accounts in full for hydrodynamic and electrostatic interactions as well as for thermal fluctuations. The solvent is modeled as a fluid of single Dissipative Particle Dynamics (DPD) beads, and the colloidal particle is modeled as a rigid body made of DPD beads. We compute the mobility and the polarizability of a single colloid and investigate systematically the effect of amplitude and frequency of the AC-fields. Even though the thickness of the Debye layer is not “thin” compared to the radius of the colloid, and the thermal fluctuations are significant, the results are in good agreement with the theoretical prediction of the Maxwell-Wagner-O’Konski theory, especially for uncharged colloids.

PACS numbers: 82.45.-h, 47.57.J-, 47.57.jd

Submitted to: *J. Phys.: Condens. Matter*

1. Introduction

Alternating electric fields (AC fields) can be used to manipulate single colloid or colloidal suspensions. This provides an attractive tool for controlling the position of individual colloid or the structure of colloidal assemblies. Since the colloids respond to external fields on relatively short time scales and in an often fully reversible way, the approach provides high flexibility in designing optimal AC pulses for a given task.

One particularly prominent example is dielectrophoresis. In dielectrophoresis, one exploits the fact that external electric fields polarize the colloids, which are then in turn driven along the direction of the field gradient. The time-averaged force acting on a particle in the AC-field $\mathbf{E} \exp(i\omega t)$ is

$$\mathbf{F}_{DEP} \sim \text{Re}\{\alpha(\omega)\} \nabla |\mathbf{E}|^2, \quad (1)$$

where $\alpha(\omega)$ is the complex polarizability of the particle. The dielectrophoretic effect can be used for trapping colloidal suspensions in “electric bottles” [1, 2], but also for selectively trapping single colloid and separating colloids or viruses by size and shape [3, 4]. It has thus many potential applications in nano- and biotechnology.

The crucial quantity in dielectrophoresis is the polarizability $\alpha(\omega)$. Assuming that the external field has a form $\mathbf{E} \exp(i\omega t)$, the effective dipole moment of a spherical particle can be written as

$$\mathbf{p} = \alpha(\omega) \mathbf{E} = 4\pi\epsilon_m K(\omega) R^3 \mathbf{E}, \quad (2)$$

where ϵ_m is the permittivity of the surrounding medium, $K(\omega)$ is the Clausius-Mosotti factor and R is the radius of the particle. For uncharged particles, the polarizability is governed by the permittivity and conductivities of the particle and the medium. For charged particles in salt solution, the electrical double layer surrounding the particle contributes significantly to the polarizability, and the dielectrophoretic response results from an intricate interplay of dipole reorientation, ion mobility, electrostatics, and hydrodynamics. The dielectric response of colloids to AC fields has attracted abiding interest for decades, but it is still not fully understood, especially in cases where the colloids have nanometer size and the electric double layer is thick, since most theoretical studies neglect thermal fluctuations and assume that the electric double layer is thin compared to the colloidal radius.

Several processes, on time scales spanning several orders of magnitude, contribute to the dielectric response of charged colloids in salt solutions. The fastest event following the sudden application of a constant electric field is the interface polarization induced by the local dielectric contrast between water and the colloid material. This happens on the GHz scale (the relaxation time of water is 17 GHz), which is instantaneous for the purpose of the present discussion. Likewise, the time for hydrodynamic flow to build up is also almost instantaneous [5]. On the MHz scale (1-10 MHz), ionic migration in the electrical double layer sets in and dominates over the molecular dipole reorientation. In this regime, the main contribution to the induced dipole moments stems from the conductivity mismatch between the particle and the solvent due to the presence of free

counterions in the solvent (Maxwell-Wagner relaxation). Finally, on long time scales up to 100Hz, a salt concentration gradient builds up along the colloid and the thickness of the double layer varies accordingly, leading to an additional source of polarization (α -polarization).

Various approaches have been proposed to explain the dielectric response of colloidal particles. In the high-frequency regime, the Maxwell-Wagner mechanism of dielectric dispersion [6, 7] has been widely discussed, which only depends on the bulk properties of the solution and the colloid. O’Konski later introduced a surface conductivity term to account for the contribution of the electric double layer [8]. The Maxwell-Wagner-O’Konski (MWO) theory has also been extended to ellipsoidal particles [9]. Theories for the low-frequency region have been developed in the Ukraine school [10] based on the standard electrokinetic model [11]. Most studies rely on the assumption that the electrical double layer is much thinner than the radius of the particle. For situations that involve thick electrical double layers and the whole frequency spectrum, numerical methods to solve the electrokinetic equations have been implemented [12, 13, 14]. In the standard electrokinetic model, ions are treated as point particles, the size effect is neglected, and a mean field approach is taken, i.e., thermal fluctuations are neglected. Moreover, linear response theory is employed in the numerical calculations, but experiments have suggested that the dielectric response becomes nonlinear already for moderate field strengths [15].

Molecular simulations can shed light on dielectrophoretic phenomena in a well-defined model system, but are still scarce [16, 17]. Such studies are numerically challenging, because two different types of long-range interactions are involved: the electrostatic and the hydrodynamic interactions. In recent years, a number of coarse-grained simulation approaches have been developed to address this class of problem. The idea is to couple explicit charges (ions, colloids) with a mesoscopic model for Navier-Stokes fluids. On the side of the fluid model, different approaches exist in the literature that range from Lattice Boltzmann (LB) methods [18, 19], Multi-Particle Collision Dynamics (MPCD) [20, 21], to Dissipative Particle Dynamics (DPD) [22, 23, 24]. In this paper, we use the DPD method. DPD is a coarse-grained simulation method which is momentum-conserving and Galilean invariant. Since it is a particle-based method, charges can be introduced quite naturally. A recent comparative study [25] indicated that the Coulomb interaction is the most time-consuming part in the simulation. The computational costs of different methods for modeling the fluid thus becomes comparable at intermediate or high salt concentrations.

In the present paper, we use DPD simulation to study the dielectric response of a single spherical colloid subject to AC fields, accounting in full for the hydrodynamic and electrostatic interactions. The remainder of this article is organized as follows: In section 2, we give a brief introduction of our simulation model. We present the simulation results on the polarizability and effects of systematically varying the properties of the external AC fields in section 3. Finally, section 4 concludes with a brief summary.

2. Model

Our simulation system has three components: The solvent, the colloidal particle and the microions. The solvent is modeled as a fluid of DPD beads without conservative interactions, i.e., we only implement the DPD dissipative and stochastic interactions without conservative forces [26]. In the following, physical quantities will be reported in a model unit system of σ (length) m (mass), ε (energy), and e (elementary charge unit). In these units, the temperature of the system is $k_B T = 1.0\varepsilon$, the number density of the fluid is $3.0\sigma^{-3}$, and each solvent bead has a mass m . The DPD friction coefficient is set to $\gamma_{DPD} = 5.0\sqrt{m\varepsilon}/\sigma$ and the cutoff radius is $r_c = 1.0\sigma$. The shear viscosity of the fluid was evaluated by analyzing pure Poiseuille flows in a microchannel by a method described in Ref. [27], and was found to be $\eta_s = 1.23 \pm 0.01\sqrt{m\varepsilon}/\sigma^2$, in good agreement with Ref. [25]. The diffusion constant of single solvent beads is measured to be $D_S = 0.66 \pm 0.02 \sigma\sqrt{\varepsilon/m}$.

The colloidal particle is represented by a large sphere which has repulsive Weeks-Chandler-Anderson (WCA)[28] type conservative interactions with the fluid particles,

$$V_{WCA}(r) = \begin{cases} 4\varepsilon \left[\left(\frac{\sigma}{r-r_0}\right)^{12} - \left(\frac{\sigma}{r-r_0}\right)^6 + \frac{1}{4} \right] & \text{for } r < r_c \\ 0 & \text{otherwise} \end{cases} \quad (3)$$

where the cutoff radius is set at the potential minimum $r_c = r_0 + 2^{1/6}\sigma$. The radius of the colloid is $R = r_0 + \sigma = 3.0\sigma$. To implement no-slip boundary conditions at the surface, a set of N_s DPD interaction sites is distributed evenly on the surface, with positions that are fixed with respect to the colloid center. These sites interact with the solvent beads through the DPD dissipative and stochastic interactions, using the same DPD friction constant as in the fluid, but twice the cutoff range. (The DPD cutoff has to be larger than the range of the WCA interaction in order to ensure that a sufficient number of fluid beads will interact with the DPD surface sites.) The total force exerted on the colloid is given by the sum over all DPD interactions with surface sites, plus the conservative excluded volume interaction,

$$\mathbf{F}_C = \sum_{i=1}^{N_s} \mathbf{F}_i^{(s)}(\mathbf{r}_i) + \mathbf{F}^{(WCA)}. \quad (4)$$

Here \mathbf{r}_i denotes the position of i -th surface sites. Similarly, the torque exerted on the colloid can be written as

$$\mathbf{T}_C = \sum_{i=1}^{N_s} \mathbf{F}_i^{(s)}(\mathbf{r}_i) \times (\mathbf{r}_i - \mathbf{r}_{cm}), \quad (5)$$

where \mathbf{r}_{cm} is the position vector of the colloid's center-of-mass. Here the excluded volume interaction does not contribute since it points towards the colloid center. The force and the torque are used to update the position and velocity of the colloid in a time step using the Velocity-Verlet algorithm. The mass of the colloidal particle is $M = 100m$ and the moment of inertia is $I = 360m\sigma^2$, corresponding to a uniformly distributed mass.

In addition, a total charge Q may be assigned to the center of the colloidal particle. To keep the whole system charge-neutral, a corresponding amount of counterions is then added to the solution. Salt microions may also be added as pairs of monovalent positively and negatively charged beads. We only consider the monovalent case where counterions or salt ions carry a single elementary charge $\pm 1e$. Charges interact by Coulomb interactions, and the Bjerrum length $l_B = e^2/(4\pi\epsilon_m k_B T)$ of the fluid is set to 1.0σ . Apart from the electrostatic interaction with other charged particles, the ions have a short-range repulsive WCA interaction with the solvent beads and each other, which has the form of Eq. (3) with $r_0 = 0$. The conservative interaction with the colloid is also given by Eq. (3) with $r_0 + \sigma = 3.0\sigma$.

Specifically, we consider neutral colloids ($Q = 0$) and colloids with positive charge $Q = +50e$ in salt-free solutions and in salt solutions with salt ion number density $\rho_s = 0.1\sigma^{-3}$. In these systems, the diffusion constant of single microions is smaller than that of solvent particles and concentration dependent, i.e., $D_I = 0.59 \pm 0.02 \sigma \sqrt{\epsilon/m}$ in systems containing only counterions, and $D_I = 0.47 \pm 0.01 \sigma \sqrt{\epsilon/m}$ in systems containing counterions and salt. Figure 1 shows a representative snapshot of a single charged colloidal particle in salt-free solution.

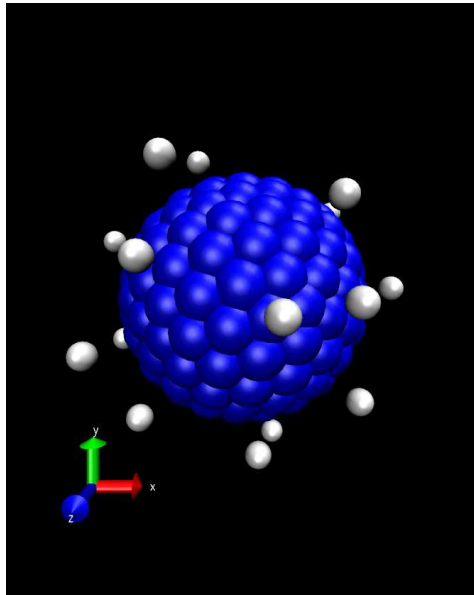


Figure 1. Snapshot of a colloidal particle in a salt-free solution. The surface sites are represented by the blue beads, and the white beads are counterions. Solvent beads are not shown here.

Our simulations were carried out using the open source package ESPResSo [29], with a slight modification that allows us to incorporate a time-dependent external electric field. A cubic simulation box of linear size $L = 20\sigma$ with periodic boundary conditions was used for all simulations. Electrostatic interactions were calculated using the Particle-Particle-Particle Mesh (P3M) method [30], and a time step of $\Delta t = 0.01\sigma \sqrt{m/\epsilon}$ was used for the integration.

As a test of our colloidal model, we have performed simulations of an uncharged colloid in a salt-free solution and measured the autocorrelation functions. Two autocorrelation functions were obtained from the simulations: the translational and rotational velocity autocorrelation functions

$$C_v(t) = \frac{\langle \mathbf{v}(0) \cdot \mathbf{v}(t) \rangle}{\langle \mathbf{v}^2 \rangle}, \quad (6)$$

$$C_\omega(t) = \frac{\langle \boldsymbol{\omega}(0) \cdot \boldsymbol{\omega}(t) \rangle}{\langle \boldsymbol{\omega}^2 \rangle}, \quad (7)$$

where $\mathbf{v}(t)$ and $\boldsymbol{\omega}(t)$ are the translational velocity and rotational velocity for the particle at time t , respectively. Figure 2 shows the simulation results averaged over ten runs with different random number generator initializations.

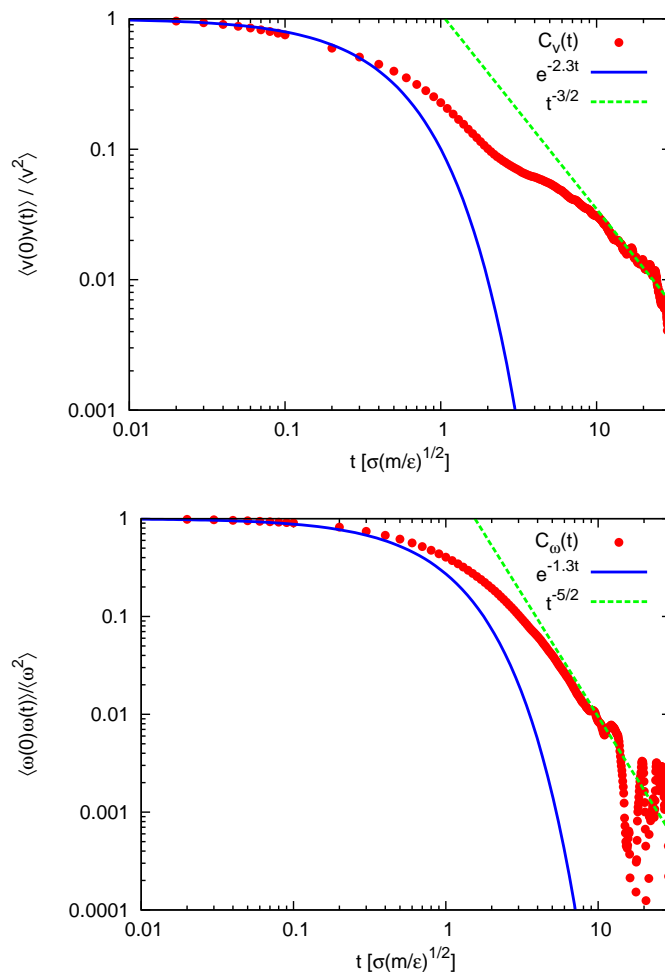


Figure 2. Translational (top) and rotational (bottom) velocity autocorrelation functions. The measurement is done for a single uncharged colloid with radius $R = 3.0\sigma$ in a salt-free solution. The temperature is $k_B T = 1.0\varepsilon$.

For short time lags, both autocorrelation functions show exponential relaxation. The decay rate can be calculated using the Enskog dense-gas kinetic theory [31, 32].

They are plotted as blue lines in Figure 2 and show reasonable agreement with the simulation data when $t < 0.1\sigma\sqrt{m/\varepsilon}$. Similar results have been obtained using MPCD simulations [33].

For long time lags, hydrodynamic effects set in and lead to a slow relaxation for autocorrelation functions of the colloidal particle [34]. This so-called long-time tail is the manifestation of momentum conservation, as the momentum must be transported away from the colloids in a diffusive manner. Mode-coupling theory predicts an algebraic $t^{-3/2}$ behavior at long times for the translational velocity and $t^{-5/2}$ for the rotational velocity [35]. The simulation results are plotted as green lines in Figure 2. The data are consistent with the theoretical prediction for $t > 10\sigma\sqrt{m/\varepsilon}$, but the rotational autocorrelation function exhibits large fluctuations for large times. This is mainly due to the fact that the statistics for long time values becomes very bad, and very long simulations are required in order to obtain accurate values.

From the velocity autocorrelation function, the diffusion constant of the colloids can be calculated using the Green-Kubo relation

$$D = \frac{1}{3} \int_0^\infty dt \langle \mathbf{v}(0) \cdot \mathbf{v}(t) \rangle. \quad (8)$$

In our case, this gives the diffusion constant $D = 0.013 \pm 0.002\sigma\sqrt{\varepsilon/m}$, which is in good agreement with the theoretical value for the diffusion constant of a Stokes sphere, $D = k_B T / (6\pi\eta_s R) = 0.0144 \pm 0.0002\sigma\sqrt{\varepsilon/m}$.

3. Results and Discussion

In this section, we report our results for single colloidal particles of radius $R = 3.0\sigma$ under alternating electric fields.

3.1. Displacement and velocity of the colloid

We start with a system containing one colloidal particle of charge $Q = +50e$, an equal amount of counterions with charge $-e$, and monovalent salt ions with a number density $0.1\sigma^{-3}$, resulting in a total of 450 negative and 400 positive microions in the solution.

Figure 3 shows the colloidal response to an AC field in x -direction with frequency $f = 0.01\sqrt{\varepsilon/m}/\sigma$ and amplitude $E_0 = 1.0\varepsilon/(\sigma e)$. After the AC field is turned on, the system is allowed to evolve for 10^6 time steps. Then the measurement is done every 10 time steps over a period of 10^6 time steps. In Figure 3, the time evolution of the electric field (top panel, Figure 3(a)) is contrasted with that of various quantities of interest (Figure 3 (b)-(e)). We will begin with discussing the displacement and velocity, shown in Figure 3 (b) and (c).

The electric field strength in this particular simulation was chosen relatively large, such that the variations of the position and velocity are above the thermal noise. The period of the applied field is $T = 1/f = 100\sigma\sqrt{m/\varepsilon}$, which is less than the diffusion time scale of the colloidal particle ($\tau_D^{(C)} = R^2/D \approx 640\sigma\sqrt{m/\varepsilon}$, where $D = 0.013\sigma\sqrt{\varepsilon/m}$

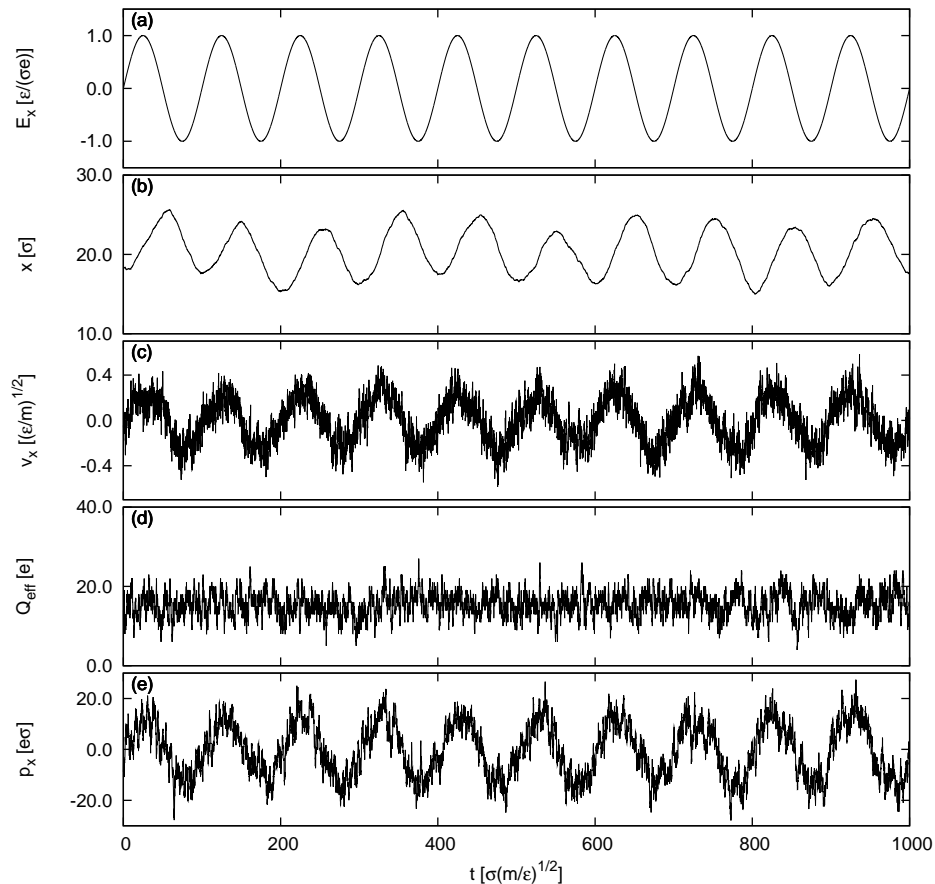


Figure 3. Dynamics of a charged colloidal particle with charge $Q = +50e$ and radius $R = 3.0\sigma$ in a salt solution (number density of salt ions $0.1\sigma^{-3}$) under the influence of an AC field with frequency $f = 0.01\sqrt{\varepsilon/m}/\sigma$ and amplitude $E_0 = 1.0\varepsilon/(\sigma e)$. (a) Instantaneous electric field. (b) Position of the particle along the field direction. (c) Translational velocity along the field direction. (d) Effective charge by counting number of ions inside the radius $r < 4.0\sigma$. (e) Dipole moment in the field direction. The effective charge and the dipole moment are discussed in section 3.2.

is the diffusion constant of the colloidal particle). On the one hand, the particle thus experiences many oscillation before diffusing over the distance of its radius. On the other hand, the period is still much larger than the diffusion time scale of the fluid ($\tau_D^{(S)} = \sigma^2/D_S \approx 1.5\sigma\sqrt{m/\varepsilon}$, where $D_S = 0.66\sigma\sqrt{m/\varepsilon}$ is the diffusion constant of solvent particles).

To rationalize the results, one may thus adopt a simplified picture where the colloidal particle is viewed as a charged sphere immersed in a viscous fluid in an AC-field. The equation of motion can be written as

$$M\ddot{x} + \gamma\dot{x} - QE_0e^{i\omega t} = 0. \quad (9)$$

The friction term is inversely proportional to the velocity and its value can be approximated using the Stokes friction $\gamma = 6\pi\eta_s R \approx 70\sqrt{m\varepsilon}/\sigma$. We solve the differential equation (9) by assuming that the position takes the form $x = Ae^{i\omega t}$, where A is a

complex number that characterizes the magnitude and phase of the oscillation. The results are

$$|A| = \frac{QE_0}{\sqrt{M^2\omega^4 + \gamma^2\omega^2}}, \quad \text{Arg}(A) = \tan^{-1}\left(\frac{\gamma}{M\omega}\right) - \frac{\pi}{2}. \quad (10)$$

Inserting the parameters of our system, we obtain that the amplitude of the position oscillation should be about 11σ , and the phase should be advanced by about $\pi/2$ compared to the applied field. Also, the amplitude of the velocity oscillation should be $0.71\sqrt{\varepsilon/m}$ and the velocity should be almost in phase with the applied field.

The simulation results shown in Figure 3 are in good qualitative agreement with the simplified theory. The position variation clearly exhibits a $\pi/2$ phase shift ahead of the applied field, while the velocity profile is in phase. However, the theory overestimates the amplitude of the oscillation. The actual amplitude of the position oscillation is about 5σ , and that of the velocity is about $0.3\sqrt{\varepsilon/m}$. One reason for this discrepancy is that counterions condense on the colloids surface, which effectively reduces the total charge of the colloids. The binding of the counterions and the colloid also increases the effective mass of the complex, which further reduces the amplitude of the oscillations. Another effect comes from the no-slip boundary condition of the colloidal particle: The fluid particles adjacent to the colloid surface are dragged along with the colloid, effectively increasing its mass.

One important quantity that characterizes the colloidal response to AC-fields is the mobility $\mu(\omega)$. In the presence of an external field $\mathbf{E}e^{i\omega t}$, the particle oscillates with the velocity $\mathbf{U}e^{i\omega t}$ with

$$\mathbf{U} = \mu(\omega)\mathbf{E}, \quad (11)$$

where the mobility $\mu(\omega)$ is a complex function of the frequency. In the simulation, the time sequence of the velocity is noisy due to the thermal fluctuation. To obtain a clear signal and extract the mobility, we apply Fourier transform to the time sequence of the velocity. Figure 4 shows the Fourier transform of the time sequence in Figure 3(c). The real and imaginary parts correspond to the in-phase and out-of-phase components of the signal with respect to the applied field. They both exhibit peaks at the frequency of the external electric field, and the peak values divided by the electric field strength give the real and imaginary part of the mobility at that frequency.

3.2. Charge distribution and dipole moment

Apart from allowing one to study the displacement and velocity of the colloidal particle, the simulations also provide valuable information about the electric double layer surrounding the colloid. During the simulation, we have collected the histograms of counterion and coion distances to the center of the colloidal particle. Figure 5(a) shows the time-averaged charge distribution around the colloidal particle. Due to the strong Coulomb interaction with the positively charged colloids, counterions accumulate close to the colloidal surface while the coions are depleted in the same region. The counterion concentration is peaked around $r = 3.2\sigma$ from the colloid center. Beyond

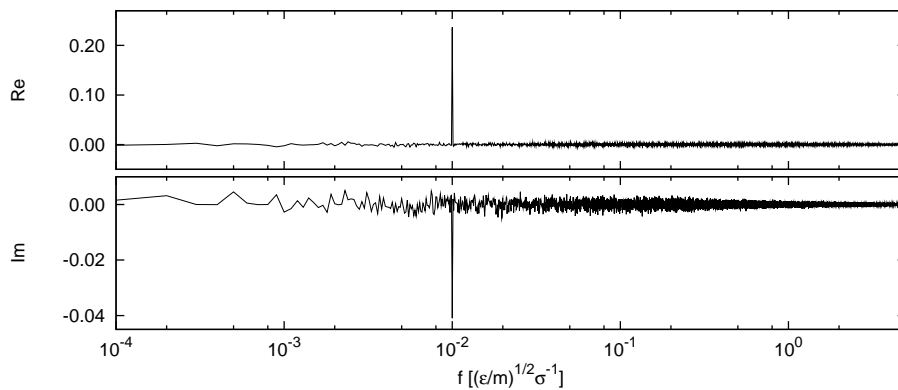


Figure 4. Fourier transform of the time sequence of the colloid velocity of Figure 3(c). The top panel shows the real part corresponding to the in-phase component of the velocity, and the bottom panel is the imaginary part corresponding to the out-of-phase component. Both the real and the imaginary parts feature peaks at $f = 0.01\sqrt{\varepsilon/m}/\sigma$, the frequency of the external field.

that distance, the counterion concentration decays rapidly to the bulk value, which is reached at around $r = 6.0\sigma$. At the same time, coions are barely present within the distance $r < 4.0\sigma$, and the concentration slowly increases to the bulk value, which is also reached at around $r = 6.0\sigma$.

The ion cloud surrounding a charged colloidal particle is commonly grouped into two regions separated by a “plane of shear”, which is defined as a hypothetical plane that separates an immobilized liquid layer and the mobile fluid. In the region inside the shear plane, also called the stagnant layer, the ions are strongly bound to the surface and have limited mobility. Due to the friction between the liquid and the particle surface, ions inside the stagnant layer follow the surface. Outside the stagnant layer, the ions are relatively free to move. The outer region up to the point where the ion concentration reaches the bulk level is called diffuse layer. The thickness of the diffuse layer is roughly determined by the Debye screening length, although it may effectively be smaller due to nonlinear effects already at moderate surface charges [36]. The Debye screening length is given by

$$l_D = \left[4\pi l_B \sum_i z_i^2 n_i(\infty) \right]^{-\frac{1}{2}}, \quad (12)$$

where z_i and $n_i(\infty)$ are i -th ion’s valence and bulk number density, respectively, and the summation is over all ion species. In our system, the Debye screening length is given by $l_D = 0.89\sigma$ in pure solution (neglecting the small contribution of the counterions).

Determining the extension of the stagnant layer is important because it contains the ions that contribute to the effective charge of the particle. In simulations, however, it is difficult to pin down the exact position of the shear plane. Different methods have been proposed in the literature [37, 38, 39, 40, 41]. One popular method is the inflection criterion [37, 38, 39]. Here one first computes the integrated counterion distribution

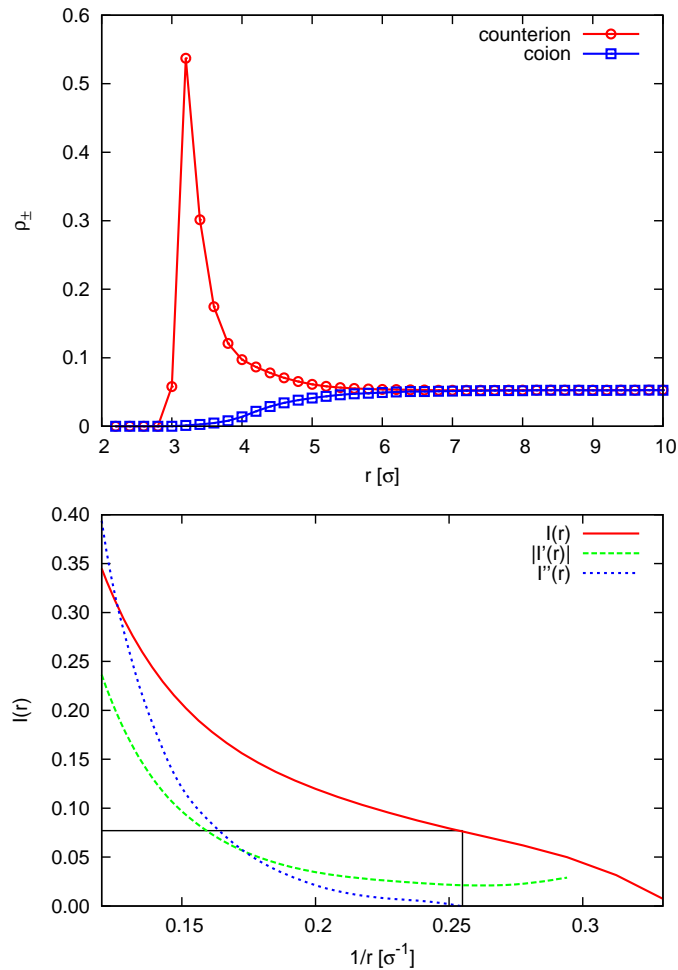


Figure 5. (a) Average number density of counterions and coions as a function of the distance to the colloid center. The average has been taken over 10^6 time steps. (b) The integrated counterion distribution $I(r)$ used to determine the cutoff radius for the effective charge. The inflection point is identified as the zero of the second derivative of $I(r)$ with respect to $1/r$.

$I(r)$ by counting the number of counterions inside a radius r with respect to the colloid center,

$$I(r) = \frac{1}{N_-} \int_0^r \rho_-(r) dV, \quad (13)$$

where $\rho_-(r)$ is the counterion number density and the normalization constant N_- is the total number of counterions. The value of $I(r)$ represents the fraction of counterions which are within a distance r from the colloid center. The cutoff radius for summing up the effective charges is then set at the inflection point (the point where the second derivative is zero) of the integrated counterion distribution plotted versus the logarithmic distance to the center. Although this criterion has originally been devised for the static case, here we will attempt to use it for the dynamic situation by applying it to the averaged counterion distribution. Figure 5(b) shows the integrated counterion

distribution. The inflection point is identified at $r = 3.9\sigma$.

Another method to determine the shear plane is to compute the colloid-ion velocity correlation [40, 41]

$$C_{ci}(r, \tau) = \langle v_c(t)v_i(r, t + \tau) \rangle - \langle v_c(t) \rangle \langle v_i(r, t + \tau) \rangle, \quad (14)$$

where $v_c(t)$ is the velocity of the colloidal particle and $v_i(r, t)$ is the velocity of ions which is located at r with respect to the colloid center. Since the motion of the colloid and the ions are strongly perturbed in the direction of the external field, we only consider the correlation in the other two directions. Figure 6 shows the correlation functions for five different r . For ions which are located in the nearest surroundings of the colloid surface, the correlation in the limit of $\tau \rightarrow 0$ is positive, indicating that those ions are moving along with the colloid. At larger distance, the ion motion becomes anti-correlated with that of the colloid, and the correlation $C_{ci}(\tau \rightarrow 0)$ turns negative. The position where the correlation first changes sign can also be viewed as a definition of the shear plane. Using this method, one locates the shear plane at $r = 3.8\sigma$, which is close to the value determined with the inflection criterion.

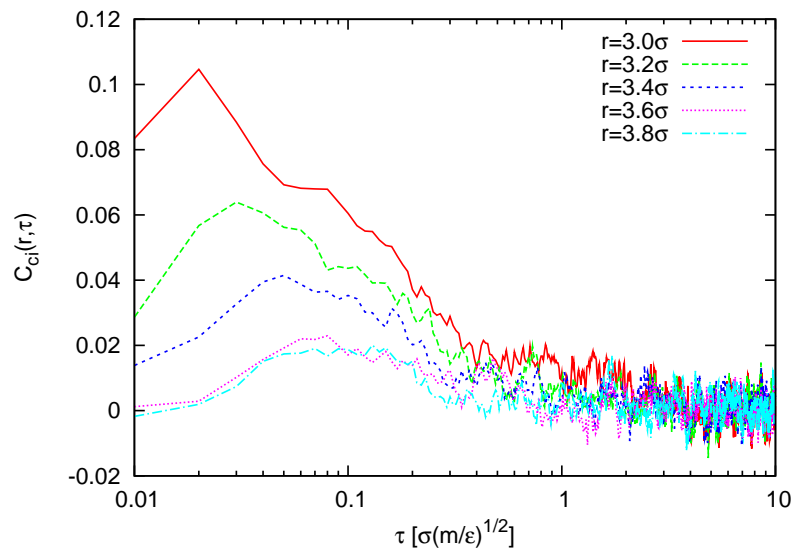


Figure 6. Colloid-ion velocity correlation function $C_{ci}(r, \tau)$. The values are averaged over two directions normal to the external field.

In order to characterize the dielectric response of the colloidal particle under external fields, we must calculate the dipole moment of the system. Whereas only the ions inside the stagnant layer contribute to the effective charge, the dipole moment also has significant contributions from the diffuse layer. Figure 5(a) indicates that the ion concentrations reach their bulk values at approximately $r = 6.0\sigma$, therefore we computed the dipole moment using a cutoff of 6.0σ from the colloid center. The time sequence of the effective charge and the dipole moment are plotted in Figure 3(d) and (e), respectively. The averaged effective charge is roughly $+15e$, corresponding to about condensed 35 counterions on the colloidal surface. The dipole moment oscillates with

the same frequency as the applied field. The complex polarizability $\alpha(\omega)$ is obtained by applying a Fourier transform to the time sequence of the dipole moment, similar to the complex mobility discussed in last section.

3.3. Influence of the strength of AC fields

Most theories on the dielectric response of charged colloids are based on the linear response theory and assume the external electric field to be weak. In our simulations, we can apply large electric fields to examine the effect of the field strength and possible nonlinear effects. In this subsection, the frequency is set at $f = 0.01\sqrt{\varepsilon/m}/\sigma$, which is in the low-frequency regime (see next section). The field strength is varied from 0.01 to $10\varepsilon/(\sigma e)$. By covering a wide range of electric field amplitudes, we are able to estimate the limit of validity of the linear response theory. Figure 7 shows the amplitudes of the colloid velocity and dipole moment as a function of the field strength.

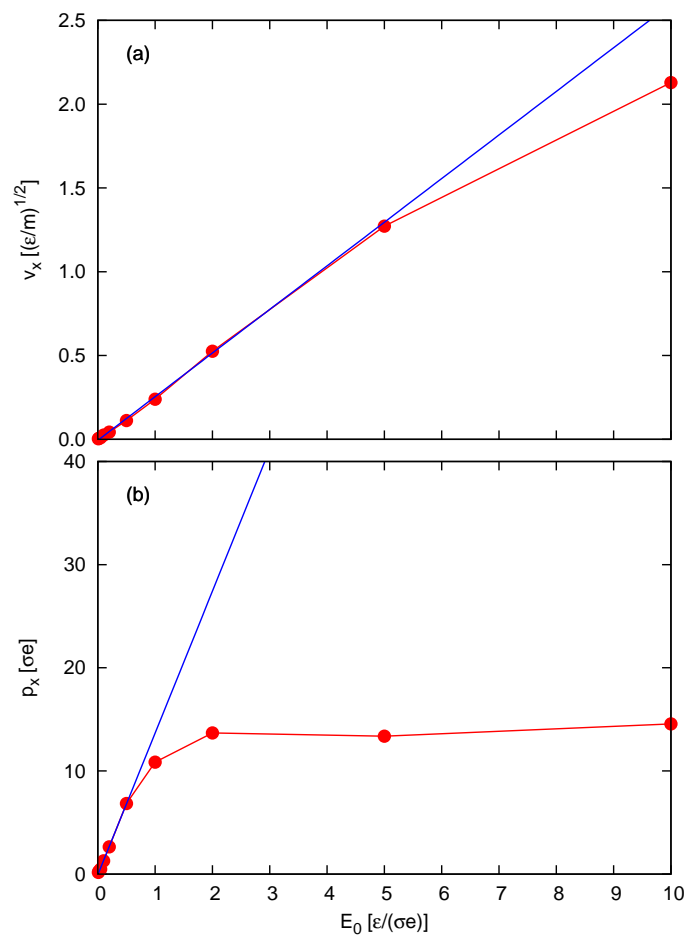


Figure 7. (a) The amplitude of the colloid velocity as a function of the field strength. (b) The amplitude of the dipole moment as a function of the field strength. The frequency of the applied field is set at $f = 0.01\sqrt{\varepsilon/m}/\sigma$.

In weak fields, the velocity grows linearly as a function of the field strength up

to $E_0 \approx 2.0\varepsilon/(\sigma e)$, corresponding to a constant mobility. For higher field strength, the growth slows down, which implies that the mobility decreases. This is different from the case of constant electric field, where the mobility is found to increase above the linear region [41]. Alternating electric fields of large field strength can excite colloidal motion with signatures of various frequencies besides the frequency of the applied field. This can be seen from the Fourier transform of the colloid velocity, shown in Figure 8, where peaks at higher frequencies appear for high field strength $E_0 = 10\varepsilon/(\sigma e)$ (see Figure 4 for comparison).

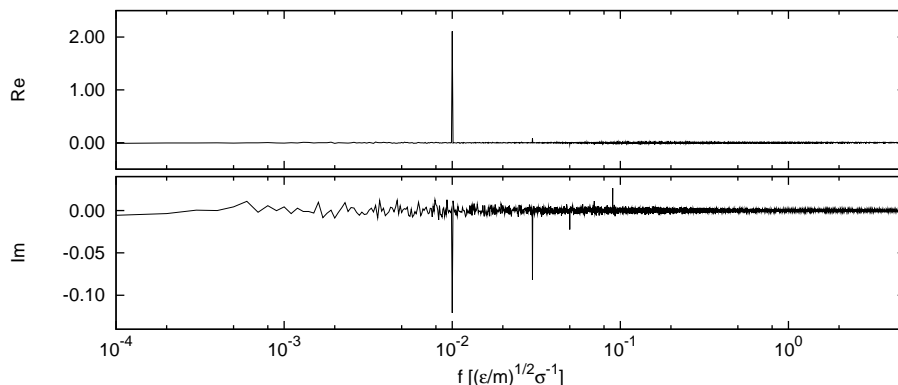


Figure 8. Fourier transform of the time sequence of the colloid velocity for a strong external field with frequency $f = 0.01\sqrt{\varepsilon/m}/\sigma$ and amplitude $E_0 = 10\varepsilon/(\sigma e)$.

Looking at the dipole moment, one finds that the deviation from the linear regime sets in at about $E_0 \approx 1.0\varepsilon/(\sigma e)$. Compared to the colloid velocity, the deviation from the linear dependence is much more pronounced for the dipole moment. This is due to the fact that the dipole moment measures how ions are distributed around the colloidal particle, and the electric double layer can easily be influenced by the external field. For intermediate field strength, the main effect of the external field is to deform the shape of the electrical double layer, as the ions in the diffuse layer are relatively mobile. The shape of the ion clouds is elongated in the field direction. Figure 9 shows the ion distribution for three different field strength, $E_0 = 0.1, 1$ and $10\varepsilon/(\sigma e)$. In the weak field region ($E_0 = 0.1$ to $1.0\varepsilon/(\sigma e)$), the change of ion distribution is small. When the field strength increases to $10\varepsilon/(\sigma e)$, the deviation becomes notable. The peak of the counterion distribution is reduced, and a second peak of coions close to the colloidal surface develops.

When the field is strong enough, it may disturb the ions inside the stagnant layer. Some of the ions originally bound to the colloidal surface will be ripped off at large enough electric field. This is demonstrated in Figure 9 where the counterion peak is reduced at higher field strength. The required field strength can be estimated by equating the force exerted by the external field and the electrostatic force from the

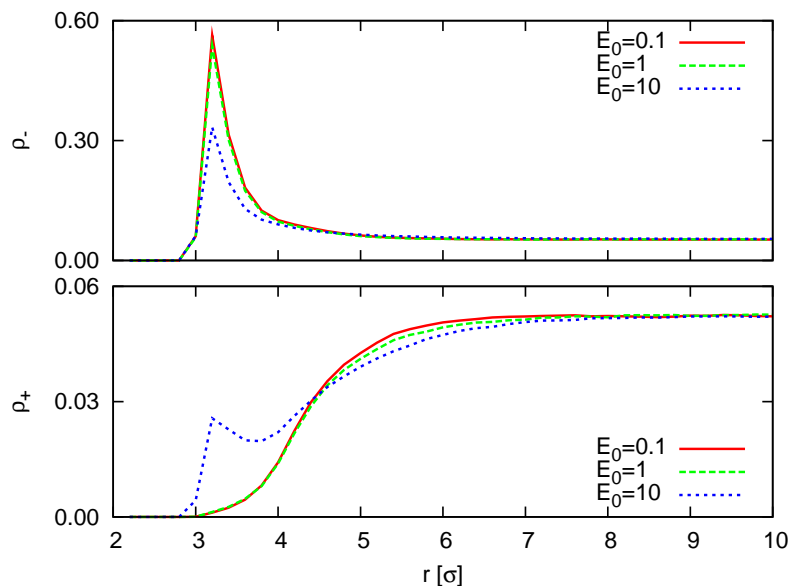


Figure 9. Comparison of the ion distribution for three different field strength $E_0 = 0.1, 1$ and $10\epsilon/(\sigma e)$. The top and bottom figures are for the counterion and coion distribution, respectively.

charged colloids.

$$E_0 = \frac{Q_{\text{eff}}}{4\pi\epsilon_m R^2 e} \approx 1.7\epsilon/(\sigma e), \quad (15)$$

where we have used $Q_{\text{eff}} = 15e$. This number seems to determine the point where the dipole moment as a function of field strength starts to level off, indicating the breakdown of the weak field assumption.

3.4. Frequency dependence

Finally, we investigate the effect of varying the frequency of the external AC field. The amplitude of the field is chosen in the linear region, $E_0 = 0.5\epsilon/(\sigma e)$. The frequency is varied from $f = 10^{-3}$ to $2.0\sqrt{\epsilon/m}/\sigma$. A separate simulation with a constant electric field is also performed to provide the reference at low-frequency limit. As in most previous simulations, the solution has a salt ion number density of $0.1\sigma^{-3}$, corresponding to the Debye length $l_D = 0.89\sigma$ in a system without counterions and $l_D = 0.87\sigma$ in a system with 50 counterions. Thus the Debye length is smaller than, but comparable to the colloidal radius ($R = 3.0\sigma$). We compare the simulations with the prediction of the Maxwell-Wagner-O’Konski (MWO) theory, which is briefly sketched in Appendix A. Even though this theory was originally developed for situations where the electric double layer is much thinner than the colloid, we shall see that it still captures the most important features of the frequency dependence on a semi-quantitative level.

We start with the easiest case of an uncharged colloidal particle, which has no electric double layer. Figure 10 shows the polarizability for an uncharged colloidal particle in salt solution with ions number density of $0.1\sigma^{-3}$. The real part of the

polarizability shows the in-phase component of the dipole moment with respect to the external field, while the imaginary part gives the out-of-phase contribution. The polarizability in the low-frequency limit has a negative real part, indicating that the induced dipole is anti-parallel to the applied field. Uncharged colloids are not surrounded by an electric double layer, and the dipole moment is induced solely by the motion of the salt ions. The positive ions move in the direction of the electric field, and tend to accumulate on the back side of the colloid, while the negative ions accumulate on the front end of the colloid. This leads to an effective dipole moment which points in the opposite direction than the external field, sometimes referred to as volume polarization [42].

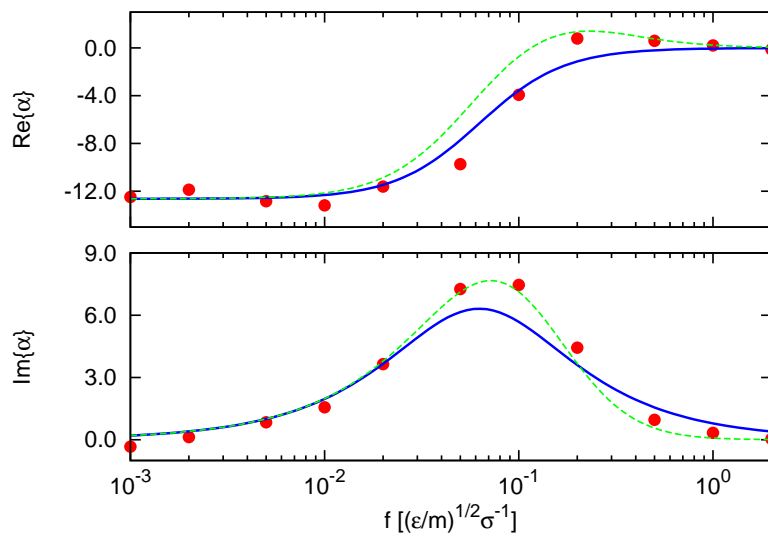


Figure 10. Real and imaginary part of the complex polarizability of an uncharged particle as a function of the frequency of applied electric field. The field strength is set in the linear region $E_0 = 0.5\epsilon/(\sigma\epsilon)$. The number density of the salt ions in the solution is $0.1\sigma^{-3}$. The points are simulation results. The solid lines give the prediction from the Maxwell-Wagner theory with the effective colloid radius $R_{\text{eff}} = 2.93\sigma$. The dashed line shows revised prediction by taking into account of inertia effects. See text for explanation.

The solid line in Figure 10 shows the prediction from the Maxwell-Wagner theory. The limiting behavior of the polarizability at frequency $f \rightarrow 0$ was obtained by an independent run in a DC field and used to calibrate the effective colloidal radius R via $\alpha(0) = 4\pi\epsilon_m K_0 R^3$, which reduces to $\alpha(0) = -R^3/2$ in our system (see Appendix A). We obtain $R_{\text{eff}} = 2.93 \pm 0.07\sigma$, which is reasonably close to the “physical” radius $R = 3.0\sigma$. The main sources of discrepancy are the soft character of the excluded volume interactions and the small size of the colloids. Having set the effective colloidal radius, we can calculate the Maxwell-Wagner prediction without further fit parameter, and the resulting curve is in quite good agreement with the simulation data (Figure 10, solid line). Most notably, the theory predicts a crossover between two regimes

which is recovered in the simulation at roughly the predicted crossover frequency. The simulations feature a slight overshoot of the polarizability in the crossover region, which can be explained by considering the inertia effect of the microions, which are not entirely negligible in our simulations. (In real systems, they are negligible.) When microions with mass are immersed in a viscous fluid, their response to the external electric fields depends on the frequency. Thus the conductivity becomes frequency-dependent. The inertia effect can be incorporated into the theory (see Appendix A) and the theory can be revised accordingly, giving the dashed line in Figure 10. It predicts small overshoots in both the real and the imaginary part of the polarizability, which are consistent with the simulation.

The situation is more complicated when the colloids are charged, due to the presence of the electric double layer. Figure 11 shows the polarizability for a charged colloid ($Q = 50e$) in salt solution (same salt concentration as before).

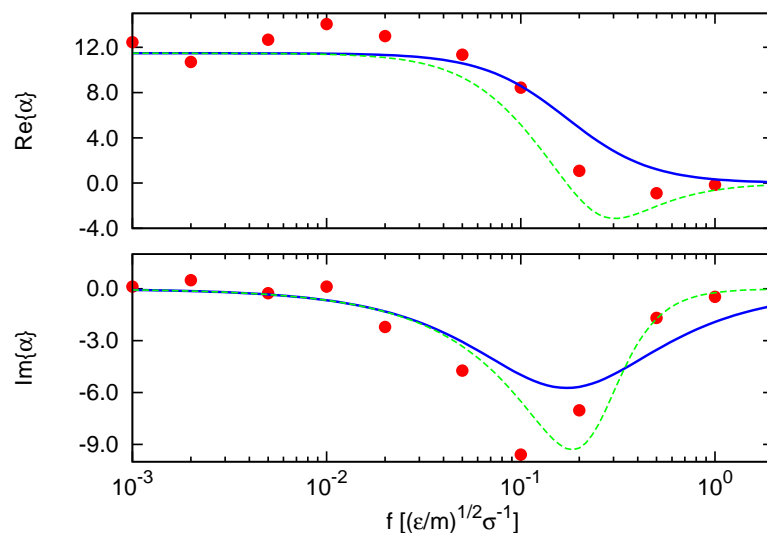


Figure 11. Same as Figure 10 for a charged colloid ($Q = 50e$). The points are simulation results. The solid lines give the prediction from the MWO theory, using an effective colloid size $R_{\text{eff}} = 2.93\sigma$ and the surface conductance $K_{\sigma} = 0.24e^2/(\sigma\sqrt{m\varepsilon})$. The dashed line shows revised prediction by taking into account of ions' inertia effect. See text for explanation.

In the low-frequency region $f < 10^{-2}\sqrt{\varepsilon/m}/\sigma$, the external perturbation is slow enough that the system can follow. The dipole moment is in phase with the applied field, as reflected by the fact that $\text{Im}\{\alpha\}$ is close to zero. The real part $\text{Re}\{\alpha\}$ is positive, in contrast to that obtained for uncharged colloids, indicating that the dipole moment points in the same direction as the applied field. In the absence of external fields, the center of the counterion cloud and the center of the spherical particle coincide, and the dipole moment is zero. If one applies an electric field, the positively charged particle moves in the direction of the field, while the negative ion cloud moves in the opposite direction. The resulting net dipole moment points in the same direction as the external

field, therefore one has $\text{Re}\{\alpha\} > 0$ in the low-frequency limit. In the opposite limit of high frequency, the colloid and the ion cloud can no longer follow the field, thus both $\text{Re}\{\alpha\}$ and $\text{Im}\{\alpha\}$ converge to zero. At intermediate frequencies $f \sim 0.1(\varepsilon/m)^{1/2}\sigma^{-1}$, the real part $\text{Re}\{\alpha\}$ crosses over from positive to zero with an overshoot below the transition frequency and a slight undershoot to negative values after the transition frequency. The imaginary part $\text{Im}\{\alpha\}$ assumes a maximum, indicating that the response is out of phase and that there is high dissipation.

According to the Maxwell-Wagner-O’Konski (MWO) theory, the effect of the electric double layer can be taken into account by introducing a surface conductance in the Maxwell-Wagner theory. Here we have determined the value of the surface conductance by calculating the $f \rightarrow 0$ limit of the polarizability from an independent simulation in a DC field, assuming that the effective radius is the same for charged and uncharged colloids. The simulation gives the surface conductance $K_\sigma = 0.24 \pm 0.07e^2/(\sigma\sqrt{m\varepsilon})$, which is consistent within the error with the theoretical estimate based on the extended MWO theory [9] (see appendix), $K_\sigma = 0.19e^2/(\sigma\sqrt{m\varepsilon})$. Using this value, we can again calculate the theoretical polarizability as a function of frequency without any fit parameter. The resulting curves without and with ion inertia effects are shown in Figure 11 with solid and dashed lines, respectively. The prediction of the MWO theory is in surprisingly good agreement with the simulations, given how questionable its validity is. The theory captures the main qualitative features, and roughly the correct crossover frequency. Similar to the uncharged case, the dielectric response at high frequency are affected by the finite mass of microions. The revised theory shows better agreement with the simulation after the transition frequency. The overshoot in the real part $\text{Re}\{\alpha\}$ may be an indication of the low-frequency dielectric dispersion [10], and further studies are required to clarify this problem.

4. Summary

We have carried out mesoscopic molecular dynamics simulations for a colloidal particle under alternating electric fields. We have accounted in full for the hydrodynamic and electrostatic interactions as well as thermal fluctuations, using Dissipative Particle Dynamics and a Particle-Particle-Particle Mesh method for evaluating Coulomb interactions.

We obtained information about the displacement and velocity of the colloidal particle. A simple classical theory is proposed to explain the simulation results at low frequency and shows positive agreement. We have also considered the contribution from the electric double layer surrounding the colloid. Two different methods, namely, the inflection criterion and the colloid-ion correlation function, were used to determine the position of the shear plane, and it was shown that they both give the same results. Furthermore, the dipole moment was calculated by integrating all contributions of ions from the colloid surface to the point where the ion concentration reaches the bulk value.

The effect of the external field strength was investigated systematically. By

computing the mobility and the polarizability for various field strength, we have examined the validity of the linear response theory. Nonlinear effects were found to set in for electric strength up to $1.0\varepsilon/(\sigma e)$, which is higher than the values reported for constant electric fields [41, 19, 43]. This can be contributed to the excitation of high-frequency modes and the stripping of the counterions that are bounded to the colloid surface.

Furthermore, the frequency dependence of the polarizability was studied for an uncharged colloid and a charged colloid in a salt solution. The simulation results were compared with the predictions of the Maxwell-Wagner-O’Konski theory. Despite the fact that thermal fluctuations are substantial and that the size of the colloids is comparable to the Debye screening length, the MWO theory performed surprisingly well, especially for uncharged colloids. The inertia effect of microions can also be incorporated into the theory to explain the high frequency behavior. For charged colloids, the theory and simulations show noticeable deviations, indicating that the thin assumption of a thin electrostatic double layer is questionable for our system.

Acknowledgments

The authors would like to thank Burkhard Dünweg, Roman Schmitz, Christian Holm, Axel Arnold, Olaf Lenz, Jens Smiatek, Peter Virnau, Shuanhu Qi and Stefan Medina Hernando. This work was funded by the Deutsche Forschungsgemeinschaft (DFG) through the SFB-TR6 “Physics of Colloidal Dispersions in External Fields”. Computational resources at John von Neumann Institute for Computing (NIC Jülich), High Performance Computing Center Stuttgart (HLRS) and Mainz University are gratefully acknowledged.

Appendix A. Maxwell-Wagner-O’Konski theory

In this appendix, we give a short introduction to the Maxwell-Wagner-O’Konski theory. More detailed information can be found in Refs. [6, 7, 8, 9].

When loss is present, the dipole moment of a particle immersed in fluids exhibits a phase lag with respect to the external sinusoidal field. A complex effective dipole moment can be written as $\mathbf{p} = 4\pi\epsilon_m K(\omega)R^3 \mathbf{E}$ (cf. Equation (2)), where the Clausius-Mossotti factor $K(\omega)$ is a complex number containing both the magnitude and the phase information about the effective dipole moment. In the Maxwell-Wagner theory, it has the form

$$K(\epsilon_p^*, \epsilon_m^*) = \frac{\epsilon_p^* - \epsilon_m^*}{\epsilon_p^* + 2\epsilon_m^*}, \quad (\text{A.1})$$

where ϵ_p^* and ϵ_m^* are the complex dielectric constants of the particle and the medium, respectively. They are defined as

$$\epsilon_p^* = \epsilon_p + \frac{K_p}{i\omega}, \quad \epsilon_m^* = \epsilon_m + \frac{K_m}{i\omega}, \quad (\text{A.2})$$

where ϵ (without the star) and K are the permittivity and conductivity, respectively. For $\epsilon_m = \epsilon_p = \epsilon$, the Clausius-Mossotti factor can be rewritten as

$$K = K_0 \frac{1 - i\tilde{\omega}}{1 + \tilde{\omega}^2} \quad (\text{A.3})$$

with

$$K_0 = \frac{K_p - K_m}{K_p + 2K_m} \quad \text{and} \quad \tilde{\omega} = \frac{3\epsilon}{K_p + 2K_m} \omega. \quad (\text{A.4})$$

In our system, we have $\epsilon_p = \epsilon_m = 1/4\pi$, $K_p = 0$, thus $K_0 = -1/2$ is negative. The conductivity of the medium K_m is related to the microion diffusion constant D_I via $K_m = n_{\text{ion}} e^2 D_I / (k_B T)$ for 1-1 electrolytes.

The classical Maxwell-Wagner theory fails to explain the dielectrophoretic properties of latex particles. Latex has a low intrinsic conductivity, but the measurement indicated that the particle conductivity is high. It was concluded that the electric double layer surface significantly contributes to the particle conductivity. This was first demonstrated by O'Konski [8]

$$K_p \rightarrow K_p + \frac{2K_\sigma}{R} \quad (\text{A.5})$$

where K_σ is the surface conductance (unit S instead of $\text{S}\cdot\text{m}^{-1}$ for conductivity) due to the electrostatic double layer. The extra contribution to the conductivity increases the Maxwell-Wagner relaxation frequency without introducing an extra dispersion (no extra extrema in the imaginary part of the polarizability). The idea is to encapsulate the contribution from the ion cloud around the colloids into one single parameter (the surface conductance). This is justified for high ionic strength, highly charged colloids and high frequencies. Another important effect of K_σ is to shift the prefactor K_0 in Eq. (A.3) towards positive values, to the point that the dielectric response changes sign if K_σ is sufficiently large.

We still need a way to obtain the surface conductance K_σ from the effective surface charge density σ in the simulation. This can be done by the procedure outlined in [9]. First, the ζ -potential is solved using the following formula [11],

$$\sigma = \frac{\epsilon_m k_B T}{e l_D} \left[2 \sinh \left(\frac{e\zeta}{2k_B T} \right) + \frac{4}{R/l_D} \tanh \left(\frac{e\zeta}{4k_B T} \right) \right]. \quad (\text{A.6})$$

The surface conductance then can be related to the ζ -potential by Bikerman's expression

$$K_\sigma = l_D \left[\exp \left(\left| \frac{e\zeta}{2k_B T} \right| \right) - 1 \right] (1 + 3m) K_m, \quad (\text{A.7})$$

where m is a dimensionless ionic drag coefficient [44, 45]. Bikerman's expression is applicable for 1-1 electrolytes, and the contribution from coions has been neglected. The ionic drag coefficient is related to the viscosity η_s and ion diffusion constant D_I ,

$$m = \frac{2\epsilon_m (k_B T)^2}{3\eta_s e^2 D_I}, \quad (\text{A.8})$$

($m = 0.092$ for our system, and $m = 0.18$ for KCl). With $Q = 50e$ and $R_{\text{eff}} = 2.93\sigma$, we obtain the surface conductance $K_\sigma = 0.19 e^2 / (\sigma \sqrt{m\epsilon})$.

The inertia effect of ions can be taken into account by considering a charged particle with charge e , mass m immersed in a viscous fluid. The equation of motion for the particle under an AC field $E_0 e^{i\omega t}$ is

$$m\ddot{x} = -\gamma\dot{x} + eE_0 e^{i\omega t}, \quad (\text{A.9})$$

where $\gamma = k_B T / D_I$ is the friction constant. After solving the equation of motion, one finds that the velocity of the particle has the form

$$\dot{x} \propto \frac{1 - i\left(\frac{m\omega}{\gamma}\right)}{1 + \left(\frac{m\omega}{\gamma}\right)^2}. \quad (\text{A.10})$$

Since the conductivity of salt solutions is proportional to the ion's velocity, it is reasonable to assume that the conductivity has the same frequency dependency

$$K_m \rightarrow K_m \frac{1 - i\left(\frac{m\omega}{\gamma}\right)}{1 + \left(\frac{m\omega}{\gamma}\right)^2}. \quad (\text{A.11})$$

The dashed lines in Figure 10 and 11 are obtained by substituting (A.11) into the Clausius-Mossotti factor (A.3).

References

- [1] M T Sullivan, K Zhao, A D Hollingsworth, R H Austin, W B Russel, and P M Chaikin. *Phys. Rev. Lett.*, 96:015703, 2006.
- [2] M E Leunissen, M T Sullivan, P M Chaikin, and A van Blaaderen. *J. Chem. Phys.*, 128:164508, 2008.
- [3] N G Green, H Morgan, and J J Milner. *J. Biochem. Biophys. Methods*, 35:89, 1997.
- [4] H Morgan, M P Hughes, and N G Green. *Biophys. J.*, 77:516, 1999.
- [5] V N Shilov, A V Delgado, F González-Caballero, J Horno, J J López-García, and C Grosse. *J. Colloid Interface Sci.*, 232:141, 2000.
- [6] J C Maxwell. *Electricity and Magnetism, vol. 1*. Dover, New York, 1954.
- [7] K W Wagner. *Arch. Electrotech.*, 2:371, 1914.
- [8] C T O'Konski. *J. Phys. Chem.*, 64:605, 1960.
- [9] D A Saville, T Bellini, V Degiorgio, and F Mantegazza. *J. Chem. Phys.*, 113:6974, 2000.
- [10] S S Dukhin and V N Shilov. *Dielectric phenomena and the double layer in disperse systems and polyelectrolytes*. Wiley, New York, 1974.
- [11] W B Russel, D A Saville, and W R Schowalter. *Colloidal Dispersions*. Cambridge University Press, Cambridge, 1989.
- [12] E H B. DeLacey and L R White. *J. Chem. Soc., Faraday Trans. 2*, 77:2007, 1981.
- [13] R J Hill, D A Saville, and W B Russel. *Phys. Chem. Chem. Phys.*, 5:911, 2003.
- [14] H Zhao and H H Bau. *J. Colloid Interface Sci.*, 333:663, 2009.
- [15] J T Zhu, W J Tian, S Zheng, J P Huang, and L W Zhou. *J. Appl. Phys.*, 102:114702, 2007.
- [16] E Salonen, E Terama, I Vattulainen, and M Karttunen. *Eur. Phys. J. E*, 18:133, 2005.
- [17] E Salonen, E Terama, I Vattulainen, and M Karttunen. *Europhys. Lett.*, 78:48004, 2007.
- [18] V Lobaskin and B Dünweg. *New Journal of Physics*, 6:54, 2004.
- [19] A Chatterji and J Horbach. *J. Chem. Phys.*, 122:184903, 2005.
- [20] A Malevanets and R Kapral. *J. Chem. Phys.*, 110:8605, 1999.
- [21] G Gompper, T Ihle, D M Kroll, and R G Winkler. *Adv. Polym. Sci.*, 221:1, 2009.
- [22] J M V A Koelman and P J Hoogerbrugge. *Europhys. Lett.*, 21:363, 1993.
- [23] P Español and P Warren. *Europhys. Lett.*, 30:191, 1995.
- [24] R D Groot and P B Warren. *J. Chem. Phys.*, 107:4423, 1997.

- [25] J Smiatek, M Sega, C Holm, U D Schiller, and F Schmid. *J. Chem. Phys.*, 130:244702, 2009.
- [26] T Soddemann, B Dünweg, and K Kremer. *Phys. Rev. E*, 68:046702, 2003.
- [27] J Smiatek, M P Allen, and F Schmid. *Eur. Phys. J. E*, 26:115, 2008.
- [28] J D Weeks, D Chandler, and H C Andersen. *J. Chem. Phys.*, 54:5237, 1971.
- [29] H J Limbach, A Arnold, B A Mann, and C Holm. *Comp. Phys. Comm.*, 174:704, 2006.
- [30] R W Hockney and J W Eastwood. *Computer Simulation Using Particles*. Adam Hilger, Bristol, 1988.
- [31] G Subramanian and H T Davis. *Phys. Rev. A*, 11:1430, 1975.
- [32] J T Hynes. *Annu. Rev. Phys. Chem.*, 28:301, 1977.
- [33] J T Padding, A Wysocki, H Löwen, and A A Louis. *J. Phys.: Condens. Matter*, 17:S3393, 2005.
- [34] B J Alder and T E Wainwright. *Phys. Rev. A*, 1:18, 1970.
- [35] J-P Hansen and I R McDonald. *Theory of Simple Liquids*. Academic Press, London, 3rd edition, 2006.
- [36] J Smiatek and F Schmid. *J. Phys. Chem. B*, 114:6266, 2010.
- [37] L Belloni. *Colloids and Surfaces A*, 140:227, 1998.
- [38] M Deserno, C Holm, and S May. *Macromolecules*, 33:199, 2000.
- [39] K Grass and C Holm. *Soft Matter*, 5:2079, 2009.
- [40] S Alexander, P M Chaikin, P Grant, G J Morales, P Pincus, and D Hone. *J. Chem. Phys.*, 80:5776, 1984.
- [41] V Lobaskin, B Dünweg, and C Holm. *J. Phys.: Condens. Matter*, 16:S4063, 2004.
- [42] J K G Dhont and K Kang. *Eur. Phys. J. E*, 33:51, 2010.
- [43] B Dünweg, V Lobaskin, K Seethalakshmy-Hariharan, and C Holm. *J. Phys.: Condens. Matter*, 20:404214, 2008.
- [44] J J Bikerman. *Trans. Faraday Soc.*, 35:154, 1940.
- [45] R W O'Brien. *J. Colloid Interface Sci.*, 113:81, 1986.